DYNAMIC 3D PET RECONSTRUCTION FOR KINETIC ANALYSIS USING PATCH-BASED LOW-RANK PENALTY

K. S. Kim [a], Y. D. Son[b], Z. H. Cho[b], J. B. Ra[c] and J. C. Ye[a,]*

[a]Bio Imaging & Signal Processing Lab., Dept. of Bio& Brain Engineering, KAIST
[b] Neuroscience Research Institute, Gachon University of Medicine and Science
[c]Image Systems Lab., Electrical Engineering, KAIST

ABSTRACT

Dynamic positron emission tomography (PET) is widely used to identify metabolism over time. However, conventional reconstruction algorithm provides a noisy reconstruction due to the lack of photon counts in each frame. Therefore, the main goal of this paper is to develop a novel spatio-temporal regularization approach that exploits inherent similarities within intra- and inter- frames. One of the main contributions of this paper is to demonstrate that such correlations can be exploited using a low rank constraint of overlapping similarity blocks. The resulting optimization framework is, however, non-smooth and non Lipschitz due to the low-rank penalty terms and Poisson log-likelihood. Therefore, we propose a novel globally convergent optimization method using the concave-convex procedure (CCCP) by exploiting Legendre-Fenchel transform.We confirm that the proposed algorithm can provide significantly improved image quality.

I. INTRODUCTION

Quantification of spatial and temporal radiotracer distribution is one of the important topics in dynamic PET studies [1]. Typically, the time activity curves (TACs) of concentration and kinetic parameters are obtained from the reconstructed images from time frames. For the case of short acquisition time, each time frame data has low photon counts, which results in very noisy reconstruction. To enhance the image quality from such photon limited data, various dynamic reconstruction algorithms have been proposed [1]. By extending the existing researches, we are interested in developing a novel spatio-temporal regularization scheme that exploits correlation structures within each intra and inter frames. In particular, this paper exploits geometric similarities in intra and inter frames. We found that a row rank constraint, which is originated from matrix completion problem in compressed sensing [2], is very useful to exploit self-similarities since the matrix rank is less sensitive to the intensity offset and is easier to capture edges, etc. In addition, we propose an overlapping patch based non-convex low rank penalty to exploit geometric self similarities. However, there are several technical challenges. First, the self-similarity structures are unknown before the final reconstruction is obtained. To address the first issue, this paper proposes a re-fineable patch search method, which iteratively refines the similarity blocks during reconstruction. Second, non-convex patch based low rank penalty term is non-smooth and the gradient of Poisson log-likelihood is non-Lipschitz, so optimization problem is non-trivial. To deal with this issue, the concave-convex procedure (CCCP) [3] is employed to convexify the concave rank prior and to make a EM-type separable likelihood function. Interestingly, the resulting subprogram have a pixel-by-pixel close form expression, which allows the algorithm converge fast. We perform simulation studies to validate the proposed algorithm. Our results demonstrate that the proposed algorithm can provide significantly improved reconstruction quality.

II. PROBLEM FORMULATION

First, we define the negative loglikelihood function from Poisson statistics as:

$$L(\mathbf{X}) \;=\; \sum_{s=1}^{S} \langle \mathbf{1}, \mathbf{A}\mathbf{x}_s \rangle - \langle \mathbf{y}_s, \log(\mathbf{A}\mathbf{x}_s) \rangle, \qquad (1)$$

where $\mathbf{1}$ denotes a vector with elements of ones, and $\mathbf{X} = [x_{ns}]_{n,s=1}^{N,S}$, $\mathbf{Y} = [y_{ms}]_{m,s=1}^{M,S}$, $\mathbf{A} = [a_{ns}]_{m,n=1}^{M,N}$ where x_{ns} denotes the unknown image at voxel n at time s; and y_{ms} represents the m-th detector measurement at time s, and a_{mn} denotes the probability that an emission photon from n-th voxel is detected at the m-th detector position, respectively.

Now, we explain our spatio-temporal patch based low rank penalty. It is well-known that a natural image has geometric self-similarities, *i.e.* some parts of the images are similar to different parts of the images. Thus, in our dynamic PET reconstruction, we are interested in imposing a patch-based low rank penalty to exploit self similarities. More specifically, to Eq. (1), we add patch-based low rank penalty for group of patches written as following:

$$\Psi_o(\mathbf{X}, \mathbf{R}) = \sum_{p=1}^{P} \lambda_p \mathrm{Rank}(\mathbf{V}_p), \qquad (2)$$

where

$$\mathbf{V}_p = \left[\begin{array}{cccc} \mathbf{R}_{p1}\mathbf{x} & \mathbf{R}_{p2}\mathbf{x} & \cdots & \mathbf{R}_{pQ_p}\mathbf{x} \end{array} \right] \in \mathbb{R}^{B \times NS}$$

where $\mathbf{R}_{pq}, q = 1, \cdots, Q_p$ denotes a size B patch extraction operator from the vectorized spatio-temporal volume of image $\mathbf{x} = \mathrm{vec}(\mathbf{X})$. We denote $\mathbf{R} = \{\mathbf{R}_{pq}\}_{p,q=1}^{P,Q_p}$ as a collection of such operator.

There exists two important issues in using the penalty in Eq. (2). First, the rank operator is not convex, we could use the nuclear norm as a convex relaxation [2]:

$$\Psi(\mathbf{V}, \mathbf{R}) = \sum_{p=1}^{P} \lambda_p \|\mathbf{V}_p\|_* \ , \tag{3}$$

where $\|\mathbf{V}_p\|_* = \sum_{k=1}^{\mathrm{Rank}(\mathbf{V}_p)} \sigma_k(\mathbf{V}_p)$ and $\sigma_k(\mathbf{V}_p)$ denotes the k-th largest singular value of $\mathbf{V}_p$. However, since it has been shown that concave penalty outperforms that convex nuclear norm [4] and the CCCP optimization framework in this paper prefers to concave prior, we use the following concave rank prior [4]:

$$\|\mathbf{V}_p\|_\nu = \sum_{k=1}^{\mathrm{Rank}(\mathbf{V}_p)} h_{\mu,\nu}\left(\sigma_k(\mathbf{V}_p)\right), \quad 0 < \nu \leq 1. \tag{4}$$

where the generalized Huber function $h_{\mu,\nu}(t)$ is defined as

$$h_{\mu,\nu}(t) = \left\{ \begin{array}{ll} |t|^2/2\mu, & \text{if } |t| < \mu^{1/(2-\nu)} \\ |t|^\nu/\nu - \delta & \text{if } |t| \geq \mu^{1/(2-\nu)} \end{array} \right. \tag{5}$$

where $\delta = (1/\nu - 1/2)\mu^{\nu/(2-\nu)}$ to make the function continuous.

Second, to construct a group of similarity patches, we need to find a similarity relationships $\{\mathbf{R}_{pq}\}_{p,q=1}^{P,Q_p}$. However, in dynamic PET, the vectorized image $\mathbf{x}$ is the very object that needs to be estimated, so $\{\mathbf{R}_{pq}\}_{p,q=1}^{P,Q_p}$ is not known *a priori*. To address this issue, we perform a re-fineable similarity searches, *i.e.* we fix a similarity mapping $\{\mathbf{R}_{pq}\}_{p,q=1}^{P,Q_p}$ using the previous estimation of $\mathbf{X}$, and find a new estimate from the updated image.

III. OPTIMIZATION FRAMEWORK

In this paper, we employ the concave-convex procedure (CCCP) [3] to minimize the resulting optimization problem.

Assuming that $\mathbf{R}$ is known, we solve the following minimization problem:

$$\min_{\mathbf{X} \in \mathbb{R}^{N \times S}} J(\mathbf{X}) \qquad \text{where} \quad J(\mathbf{X}) = L(\mathbf{X}) + \Psi(\mathbf{X}, \mathbf{R}) \ . \tag{6}$$

Here, the gradient of $L(\mathbf{X})$ is non-Lipschitz, and each element of $\mathbf{X}$ should be nonnegative. Now we show how CCCP framework work for our optimization framework.

Note that the negative loglikelihood term $L(\mathbf{X})$ for the Poisson noise in Eq. (1) is convex. To apply the CCCP, we use a concave coordinate transform. More specifically, we define $z_{mn}^s = \log(a_{mn}x_{ns})$. Then, $-\log\left(\sum_{n=1}^N a_{mn}x_{ns}\right) = -\log\left(\sum_{n=1}^N e^{z_{mn}^s}\right)$, which becomes concave with respect to $\{z_{mn}^s\}_{n=1}^N$. Therefore, we have

$$L(\mathbf{X}) \quad = \quad \min_{\mathbf{c}} L_c(\mathbf{X}, \mathbf{c}),$$

where

$$L_c(\mathbf{X}, \mathbf{c}) = \sum_{s=1}^{S} \mathbf{A}\mathbf{x}_s + \langle \mathbf{c}_s, \log \mathbf{c}_s \rangle - \langle \mathbf{c}_s, \log(\mathbf{A}\mathbf{x}_s) \rangle. \tag{7}$$

In the case of the patch-based rank penalty, we use the generalized Huber function in Eq. (5). Here, $|t|^2/\mu - h_{\mu,\nu}(t)$ is strictly convex. Therefore, the Legendre-Fenchel transform tells us that there exist $g_{\mu,\nu}$ such that

$$h_{\mu,\nu}(t) = \min_s \{|s-t|^2/\mu + g_{\mu,\nu}(s)\}. \tag{8}$$

The corresponding rank penalty for a matrix $\mathbf{V}$ is given by

$$\begin{aligned} \|\mathbf{V}\|_{h_{\mu,\nu}} \quad &= \quad \sum_{k=1} h_{\mu,\nu}(\sigma_k(\mathbf{V})) \\ &= \quad \min_{\mathbf{W}} \left\{ \frac{1}{\mu}\|\mathbf{V} - \mathbf{W}\|_F^2 + \|\mathbf{W}\|_{g_{\mu,\nu}} \right\} \end{aligned} \tag{9}$$

where $\|\mathbf{W}\|_{g_{\mu,\nu}} = \sum_{k=1} g_{\mu,\nu}(\sigma_k(\mathbf{V}))$. Chartrand [4] showed that $g_{\mu,\nu}(s)$ is convex when $\nu = 1$, but in general it is not convex. However, even when $g_{\mu,\nu}$ is non-convex and does not have a close form expression, there exist a close form expression for the minimizer of Eq. (8) given as

$$\mathrm{shrink}_\nu(t, \mu) = \max\{0, |t| - \mu|t|^{\nu-1}\}t/|t| \ . \tag{10}$$

Now, using Eq. (7) and Eq. (9), we have the following minimization problem:

$$\min_{\mathbf{x}, \mathbf{c}, \{\mathbf{W}_p\}_{p=1}^P} L_c(\mathbf{X}, \mathbf{c}) + \sum_{p=1}^{P} \lambda_p \left\{ \frac{1}{\mu}\|\mathbf{V}_p - \mathbf{W}_p\|_F^2 + \|\mathbf{W}_p\|_{g_{\mu,\nu}} \right\}.$$

One of the main advantage of the proposed CCCP framework is that each subproblem has close form solutions. Here, we describe them in detail.

III-A. Minimization with respect to $\mathbf{W}_p$

First, note that the minimization problem is independent to $L_c(\mathbf{X}, \mathbf{c})$. Moreover, the problem can be decomposed for each patch by patch. More specifically, we have

$$\mathbf{W}_p^{(k+1)} = \arg\min_{\mathbf{W}} \left\{ \frac{1}{\mu}\|\mathbf{V}_p^{(k)} - \mathbf{W}\|_F^2 + \|\mathbf{W}\|_{g_{\mu,\nu}} \right\}. \tag{11}$$

Using the shrinkage relationship in Eq. (10), the close form solution for Eq. (11) is given by

$$\mathbf{W}_p^{(k+1)} = \mathbf{L}\mathrm{shrink}_\nu(\mathbf{\Sigma}, \mu)\mathbf{U}^H,$$

where $\mathrm{shrink}_\nu(\mathbf{\Sigma}, \mu)$ denotes an element by element singular value shrinkage operator.

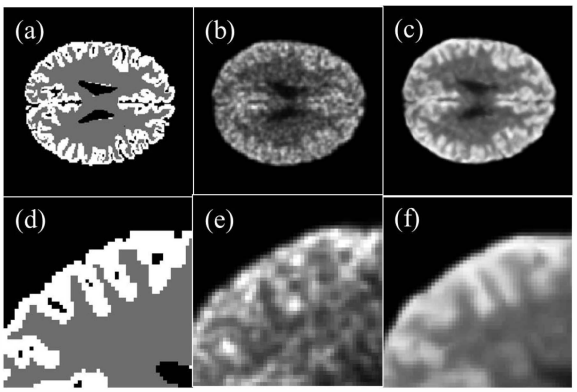

Fig. 1. Reconstruction images of (a)(d) Ground truth, (b)(e) Gaussian smoothing of conventional OSEM, and (c)(f) the proposed algorithm.

III-B. Minimization with respect to c

Using the constraint $\sum_{n=1}^{N} c_{mn}^{s} = y_m$, we have the following close form solution for the constrained optimization problem:

$$c_{mn}^{s(k+1)} = y_{ms} \frac{a_{mn} x_{ns}^{(k)}}{\sum_{n'=1}^{N} a_{mn'} x_{n's}^{(k)}}, \quad \forall\, m, n, s\ . \tag{12}$$

III-C. Minimization with respect to X

Finally, for given $\mathbf{c}^{(k+1)}$ and $\mathbf{W}^{(k+1)}$, we can obtain a close form solution for update of $\mathbf{X}^{(k+1)}$. We calculate a fixed point equation of the gradient of the cost function with respect to x_{ns}. Then, the close form solution is given by

$$x_{ns}^{(k+1)} = \frac{-b_{ns} + \sqrt{(b_{ns})^2 + 4 d_{ns} x_{ns}^{EM} \sum_{m=1}^{M} a_{mn}}}{2 d_{ns}}, \tag{13}$$

where

$$x_{ns}^{EM(k+1)} = \frac{c_{mn}^{s(k+1)}}{\sum_{m=1}^{M} a_{mn}}, \tag{14}$$

and

$$d_{ns} := \frac{1}{\mu} \sum_{p \in I_{ns}} \lambda_p, \quad b_{ns}^{(k+1)} = \sum_{m} a_{mn} - \frac{1}{\mu} \sum_{p \in I_{ns}} \lambda_p w_{p,ns}^{(k+1)}.$$

Note that the solution is always non-negative, and our update equation is pixel-by-pixel update similar to OSEM algorithm, and guarantees the global convergence.

IV. EXPERIMENTAL RESULTS

To validate our proposed algorithm, we first generated 15 frames of low photon count emissions in grey and white matters using the Monte-Carlo simulation. We then compared reconstruction images using Gaussian smoothing of the conventional OSEM and the proposed algorithm. In Fig. 1, our proposed algorithm provided significantly enhanced details of shapes and the boundaries of the grey matters are clearly visible. In addition, we calculated TACs of the Gaussian smoothing image and the proposed image in Fig. 2. Results showed that our proposed method has less errors compared to Gaussian smoothing. Finally, to demonstrate the convergence of the algorithm, the negative loglikelihood in Eq. (1) were calculated as shown in Fig. 3.

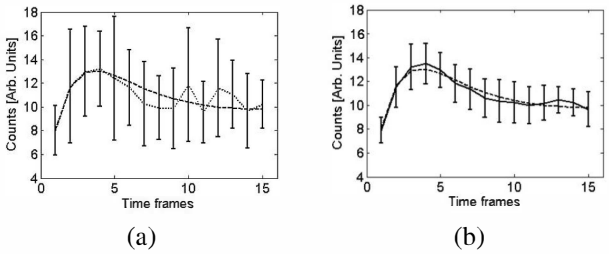

Fig. 2. TACs of (a) the Gaussian smoothing image and (b) the proposed image.

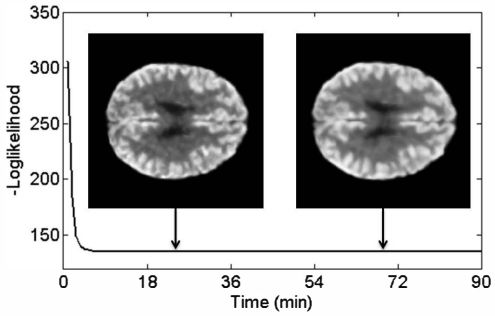

Fig. 3. Negative loglikelihood by iteration.

V. CONCLUSIONS

In conclusion, we proposed a dynamic PET reconstruction using non-convex low rank patch based regularization and derived a globally convergent algorithm using CCCP procedure. In simulation experiment, our proposed algorithm provided significantly improved images as well as accurate time activity curves.

ACKNOWLEDGMENT

This research was supported by by the Converging Research Center Program through the National Research Foundation of Korea (NRF) funded by the Ministry of Education, Science and Technology (2012K001492).

VI. REFERENCES

[1] A. Rahmim, J. Tang, and H. Zaidi, "Four-dimensional (4D) image reconstruction strategies in dynamic PET: beyond conventional independent frame reconstruction," *Medical Physics*, vol. 36, pp. 3654–3670, 2009.

[2] E. Candès and B. Recht, "Exact matrix completion via convex optimization," *Foundations of Computational Mathematics*, vol. 9, no. 6, pp. 717–772, 2009.
[3] A. Yuille and A. Rangarajan, "The concave-convex procedure," *Neural Computation*, vol. 15, no. 4, pp. 915–936, 2003.
[4] R. Chartrand, "Nonconvex splitting for regularized low-rank sparse decomposition," *Los Alamos National Laboratory Report: LA-UR-11-11298*, 2012.